

Telechelic Star Polymers as Self-Assembling Units from the Molecular to the Macroscopic Scale

Barbara Capone,^{1,*} Ivan Coluzza,¹ Federica LoVerso,² Christos N. Likos,¹ and Ronald Blaak¹

¹*Faculty of Physics, University of Vienna, Boltzmannngasse 5, A-1090 Vienna, Austria*

²*Institut für Physik, Johannes-Gutenberg-Universität Mainz, D-55099 Mainz, Germany*

(Received 9 August 2012; published 4 December 2012; corrected 11 January 2013)

By means of multiscale molecular simulations, we show that telechelic-star polymers are a simple, robust, and tunable system, which hierarchically self-assembles into soft-patchy particles and mechanically stabilizes selected, open crystalline structures. The self-aggregating patchy behavior can be fully controlled by the number of arms per star and by the fraction of attractive monomeric units at the free ends of the arms. Such self-assembled soft-patchy particles while forming, upon augmenting density, gel-like percolating networks, preserve properties as particle size, number, and arrangement of patches per particle. In particular, we demonstrate that the flexibility inherent in the soft-patchy particles brings forward a novel mechanism that leads to the mechanical stability of diamond and simple cubic crystals over a wide range of densities, and for molecular sizes ranging from about 10 nm up to the micrometer scale.

DOI: [10.1103/PhysRevLett.109.238301](https://doi.org/10.1103/PhysRevLett.109.238301)

PACS numbers: 82.70.-y, 05.10.-a, 81.16.Fg, 83.80.Uv

The current design of materials in the nanometer scale with its vast applications for, e.g., molecular electronics, therapeutic vectors, and diagnostic imaging agent carriers, or photonics, focuses on the fabrication of a variety of organic and inorganic building blocks with different sizes and shapes, which are chemically decorated with discrete and specific interaction sites. Over the past years, functionalized particles gained an important role as building blocks for various materials [1–5], raising the need for fabrication techniques that are both simple enough, and, at the same time, allow for a large-scale and reliable production of these particles. State of the art methods for the synthesis of such particles include lithography [6,7], microfluidics [8], or glancing angle deposition [9,10]. However, shape-specific particle fabrication becomes more challenging when the particle has to be decorated by a large number of patches or if the shape and location of the patches has to be tuned and controlled with extremely high precision.

In this work, we show that diblock copolymer stars are a macromolecular system that allows for an extremely well-controlled production of novel particles with a potentially unlimited number of patches. Diblock copolymer stars are star polymers whose arms are characterized by dual physical or chemical functionalities. In particular, each arm is an amphiphilic AB diblock with a solvophilic, athermal part A that is grafted in the center of the star, followed by a solvophobic, thermosensitive part B . Accordingly, we adopt the terminology *telechelic star polymers* (TSP) throughout. The solvophilic nature of the interior monomers results in a preferential maximization of the exposure to the solvent, whereas the solvophobic tail monomers tend to minimize their interaction with the same. By employing a coarse-grained approach, we surpass the molecular size limits of previous computational and theoretical approaches [11,12] and we demonstrate how, for extremely large and very dense systems (up to 10^7 monomers), by

modifying the chemical composition of the polymer chains and the number of arms, it is possible to obtain stable soft-patchy particles that survive in their self-assembled patchy state up to high concentrations. In contrast to the conventional hard-patchy colloids [13], the patches here are formed by the self-association of flexible polymer chains, which can recombine and rearrange. The process of self-assembling in patches is then succeeded by a hierarchical assembly on an even larger scale. The properties of TSP's are determined by the interactions between the monomers and the solvent, the percentage α of solvophobic monomers per arm, and the number of arms f . In what follows, each of the f arms is composed by a total of M_A solvophilic and M_B solvophobic monomers.

By using a first-principles coarse-graining procedure based on a soft-effective segment picture [14] (see Supplemental Material [15]), we represent the TSP's by modeling the AB blocks of every arm with n_A and n_B blobs. Each individual blob (or effective segment) contains a number $m_A = M_A/n_A$ or $m_B = M_B/n_B$ monomers, respectively. As was shown in Refs. [14,16], once the set of potentials characteristic for a specific AB diblock at a given temperature is computed, any asymmetry ratio $\alpha = M_B/(M_A + M_B)$ can be obtained by adjusting the numbers n_A and n_B of blobs in each arm. Choosing the number of monomers in every blob large enough to be in the scaling regime enables us to obtain reliable properties and a general behavior of the polymeric particles, allowing thus for a mapping onto experimental systems. The underlying microscopic molecules analyzed here are formed by $M = 10\,000$ monomers per arm, which are represented in our approach by at least $n_{\min} = 50$ blobs. Additional simulations of molecules with $M = 1000, 2000, 5000$, and 7000 monomers per arm have produced identical results, therefore implying the scalability of the properties of the system with the size of the molecule, as long as each arm has

sufficient monomers to be in the scaling regime. To extract the set of effective potentials representing the effective segments within the arms, full monomer simulations of diblock copolymers were performed at zero density employing a lattice model. In the full monomer representation, the solvophilic part was represented by self avoiding random walks, while to represent the solvophobic part we used a square-well interaction between monomers, adjusting the well depth so that the B blocks of the chains lie slightly below their Θ temperature. The potentials, extracted taking into account all the many-body interactions acting in the system [14,17], are depicted in Fig. 1.

We first characterize the system in the infinite dilution limit. To this end, the self-aggregation properties of a single molecule are classified as a function of its number of arms f and the percentage α of attractive monomers per arm. Hereto, single molecule simulations are performed within the coarse-grained approach described above for various combinations of $f \in [2, 20]$ and $\alpha \in [0.1, 0.8]$. The single-molecule conformational diagram showing the soft patchy particle nature of the TSP's and the tunability of the number of patches p as a function of f and α is presented in Fig. 2. It reveals that molecules with $\alpha \lesssim 0.3$ show no sign of

self-aggregation, whereas such a behavior can clearly be identified for $\alpha \gtrsim 0.3$. For given (f, α) values, molecules self-assemble into patchy particles characterized by as many as six patches in the parameter range considered. The number of patches that are formed, and the concomitant anisotropy of the particles, can be precisely tuned by choosing an appropriate combination of (f, α) . As $\alpha \rightarrow 1$, we expect of course the TSP's to turn into spherically symmetric, compact colloids, but the region in which this happens lies beyond the range shown in Fig. 2. Previous full monomer works on TSP's with much shorter arms ($M \lesssim 30$) [11,18] showed that, for a certain range of the (f, α) parameters, these molecules exhibit similar behavior as the stars with $M = 10000$ monomers per arm: they self-assemble into structures with single or multiple assembly sites that were named single or multiple "watermelons." The full monomer analysis showed that the single collapsed watermelon conformation becomes unstable for short chains at fixed temperature when increasing the number of arms ($f > 6$) in favor of multiple watermelon structures, identical to the patchy particles found here.

Recently, it has been demonstrated that linear block copolymers have the ability to assemble into micelles or

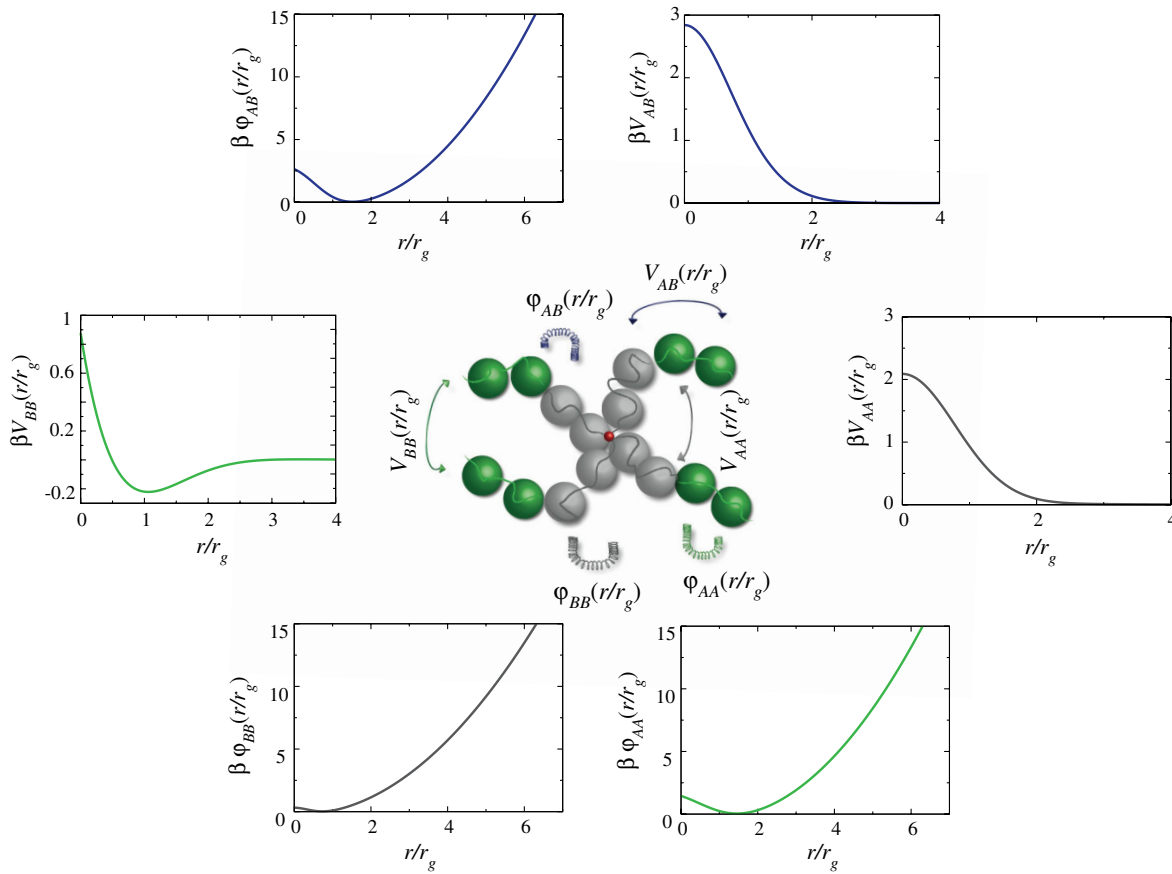


FIG. 1 (color online). The nonbonded potentials V_{AA} , V_{AB} , and V_{BB} , and the tethering potentials ϕ_{AA} , ϕ_{AB} , and ϕ_{BB} , as indicated on the axes, acting between the various blobs of type A and B . Color coding of the blobs: light gray or gray (solvophilic), dark gray or green (solvophobic), central point or red (anchor point). The radius of gyration of the A and B blobs is the same and labeled as r_g .

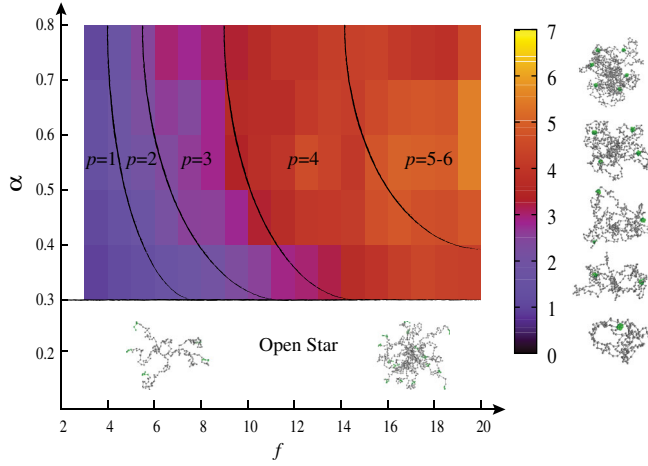


FIG. 2 (color online). Single-molecule conformational state diagram of TSP's, shown as a function of the number of arms f and asymmetry ratio α . The number of multi-arm patches p is indicated on the plot. Stars with $\alpha \lesssim 0.3$ remain in an open configuration.

cylinders decorated by patches [19,20]. In Ref. [20], it was shown that an increase of the density of block copolymers in solution induces a growth in the patchy aggregate, whose size and patchiness therefore change with concentration. If one aims at producing robust soft patchy particles, however, the stability of the aggregate formed by block copolymers should be tested against the density of copolymers in solution. Therefore, to assess to which extent TSP's are stable, self-aggregated patchy particles that maintain their zero-density properties even in the semi-dilute and concentrated regimes, simulations at finite density have been performed for a number of selected (f, α) combinations. We spaced our simulations over a wide range of densities, starting from $0.5\rho^*$ to $10\rho^*$, where $\rho^* = 3/(4\pi R_g^3)$ is the overlap density of TSP's having gyration radius R_g . Simulations of $N \in [100, 250]$ stars made of $f \in [3, 20]$ arms that have a percentage of attractive monomers $\alpha \in [0.2, 0.8]$ have been performed.

For every density, we quantify the properties of the single particle and of the whole solution by performing both a cluster analysis and a topological analysis by means of the Euler characteristic [15]. Both approaches consistently reveal that the finite density aggregation phenomenon is a consequence of the structure of the local intraparticle aggregation that leads to the formation of patches. As concentration grows, interstar patch merging leads to the formation of low density percolating gels or networks, see Fig. S3 of the Supplemental Material [15]. The cluster analysis of the gel shows that the zero density single star properties, i.e., the average number of patches per star, the average angle between the patches, and the distance of the patches from the centre of the star, together with the fluctuations over the average values, are unaffected by the density of stars in solution. This is further

supported by the topological analysis [15]. Thus, even in the random gel, the zero-density self-aggregation properties of TSP's remain unaffected.

TSP's with a given patchiness thus emerge as novel *candidates* for the stabilization of ordered, crystalline states possessing local coordination compatible with the given particle anisotropy. We therefore consider two target crystals to assess the large scale self-assembling properties of TSP soft patchy particles, namely a diamond and a simple cubic crystal. Fourfold-coordinated TSP's are compatible with a diamond lattice, whereas sixfold-coordinated ones are a natural choice to obtain stable simple cubic crystals. Hard core patchy particles have proven to be an extremely versatile system for the synthesis of a wide variety of crystals; however even if several geometries of patches have been considered, some crystals have been found to be stable only within a very small interval of the parameters range, i.e., number of patches, strength of the attractive potential and temperature [4,21].

We found that the flexibility both in the stiffness of the core and in the localization of the patches on the pre-assembled, crystalline array of particles is a major advantage when patches undergo large-scale self-assembly processes. This flexibility has its main origin at the entropically driven fluctuations of the self-avoiding blocks of the arms. In particular, we placed the anchoring points of the TSP's at the positions of various perfect lattices (simple cubic, diamond, fcc, bcc) and their arms at various different initial single-particle equilibrated configurations and we performed very long simulations (lasting at least 10^{12} Monte Carlo cycles), letting the system free to equilibrate and evolve. Since the diamond lattice has a coordination of four neighbors, the natural choice for the (f, α) parameters of the constituent stars, are f in the range $[10, 16]$ and $\alpha \in [0.4, 0.8]$, values for which, at zero density, stars self assemble in four patches. Similarly, the simple cubic requires stars with $f = 20$ and $\alpha \in [0.5, 0.7]$, that self assemble in six patches at low density. However, in principle, stars could stabilize different crystal structures whose coordination number is compatible with the number of arms per star instead of with the number of patches that are formed at zero density. If the stabilization mechanism is dominated by the attractive monomers at the end of every arm per star, for example for the range of f that assembles in four patches, then indeed the diamond, bcc and fcc crystals (with coordination numbers of 4, 8, and 12, respectively), could be all viable candidates. To reduce the computational cost, we considered the scenarios corresponding to $f = 15$ and $\alpha = 0.6$ and $f = 15$ and $\alpha = 0.4$ for the fourfold-coordinated TSP's, and $f = 20$, $\alpha = 0.5$ for the sixfold-coordinated ones at a wide range of reduced densities $\rho/\rho^* \in [1.3, 10]$.

For all the densities analysed, both bcc and fcc crystals melted within the simulation time; on the contrary, the

diamond and simple cubic crystals remain mechanically stable respectively for the four- and sixfold-coordinated particles. A mean square displacement (MSD) analysis of the crystals (not shown) has been performed to assess the stability of the system; both the bcc and fcc displayed a continuously growing MSD, while the diamond and simple cubic crystals analysed show saturation to a plateau at long times. A cluster analysis performed on the crystal shows that the zero density single-particle properties are preserved in the crystalline phase for a wide range of densities. In particular, the average number of patches (patchiness, p), the bond angles between the segments connecting the anchoring point to two different patches (interpatch angle ω) as well as the distance from the anchoring point to the center of mass of the patch (patch extension L) were fully preserved in the crystalline phase for a wide range of dilution with respect to the values they have at infinite dilution, see Tables ST1 and ST2 of the Supplemental Material [15].

Tetrahedrally coordinated TSP's, such as the ones with $f = 15$ considered here, mechanically stabilize prearranged diamond crystals by merging the attractive patches belonging to molecules on neighboring sites, and sixfold-coordinated TSP's, such as the ones with $f = 20$ considered, stabilize simple cubical crystals via a similar mechanism. The flexibility in the location of the patches and in the distance between the patches and the anchor point induces a novel mechanism for the stabilization of the two crystals. Patches are not only merging among the first neighbors but involve further stars all the way to the third neighbors. Such a preference can be understood by taking into account the fact that the TSP's maintain their patchy structures at all crystal densities; hence, with decreasing lattice spacing the stars are forced to pack by pushing the bulky self-avoiding part of the arms into the empty spaces around each lattice site. For the diamond crystal, such spaces are distributed with tetrahedral symmetry, compatible with the natural angular arrangement of the patches formed by each star. Once pushed into such spaces, the attractive patches can interact with the patches belonging to the other stars present in the same volume, which correspond up to the third neighbors. Similarly to the diamond, the simple cubic crystal is also stabilized by the packing of the self-avoiding branches of the TSP's, which reach patches in the neighboring cells. Snapshots of a typical diamond crystal formed for $(f, \alpha) = (15, 0.4)$ and of a stable simple cubic crystal formed by $(f, \alpha) = (20, 0.5)$ are shown in Fig. 3. In the figure, the diamond and the simple cubic arrangements of the centres of the stars, surrounded by a high density cloud of polymers, are clearly visible.

The same mechanism is also responsible for the rapid melting of the bcc and fcc crystals, which are not compatible neither with the packing of the self-avoiding arms and lack the ability to create local environments that favor a

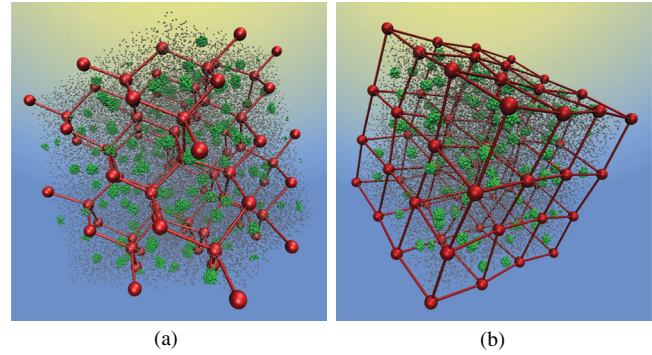


FIG. 3 (color online). Stable diamond lattice (a) and simple cubic crystal (b) obtained respectively for the $f = 15$, $\alpha = 0.4$ and $f = 20$, $\alpha = 0.5$ systems. The red lines connecting the anchor points of the stars, are a guide to the eye, drawn to stress the four fold coordinated diamond lattice structure and six fold coordinated simple cubic structure. Color coding as in Fig. 1 (Bonds not shown).

tetrahedral arrangement. This effect can be observed by monitoring the preference for first, second, and third neighbor patch fusion at increasing densities. Moreover, and in contrast to the case of athermal star polymers and chains, the radius of gyration of the star is only very weakly affected by increasing the concentration. In fact, even at the infinite dilution the size of the multi-patch TSP's considered here is significantly smaller than that of their athermal counterparts with the same f and number of monomers per arm. Concomitantly, no further shrinkage is necessary as the density grows and the TSP's maintain the size and form they have at the infinite dilution limit.

The lattices that have turned out to be mechanically stable during the simulation time have been prearranged. However, during the long simulations, the patches themselves have undergone extensive rearrangements and the particle centers have moved from their initial positions, with their mean-square displacements reaching a plateau. Thus, although the thermodynamic stability of the crystals has not been demonstrated by, e.g., a free energy calculation, the number of competing candidate structures has been reduced, since other typical candidates (e.g., bcc and fcc) have melted away. There is thus a preference for tetrahedral ($p = 4$) or sixfold ($p = 6$) coordination in the crystals, depending on the patchiness of the soft particles. We also point out that we have *not* addressed at all the issue of nucleation of those crystals out of the fluid or the gel, since it lies beyond the scope of the current contribution.

We have shown that telechelic star polymers are extremely tunable and versatile building blocks that have the ability to hierarchically self-assemble into soft patchy particles, which organize themselves into complex structures. Using advanced computational methods we fully characterize the self-organization properties of telechelic star polymers from zero density all the way up to high

concentration regimes, where we observe stable diamond and simple cubic crystals over a wide range of densities. At low density the stars self-aggregate into particles decorated by a number of patches that is completely tunable by choosing different combinations of the functionality f of the stars and on the percentage α of attractive monomers per arm. Results remain invariant within the limits $M \in [10^3, 10^4]$ monomers per star, implying their scalability with molecular size. In addition, the major findings of our work rest on the competition between the enthalpic attractions between the solvophobic, terminal blocks and the self-avoiding central ones. Therefore, we expect that our results will remain essentially unaltered over a substantial range of temperatures $T < T_\Theta$, provided the terminal monomers do not reach the fully collapsed regime. In general, as the temperature is lowered, the solvophobic tails will collapse onto a decreasing number of patches and the “phase boundaries” in Fig. 2 will move to the left in f and down in α . As such, TSP’s might prove to be excellent candidates for realizing the “pinched phase diagram” predicted and analyzed for the case of hard patchy particles [22,23].

State of the art of technology allows us to fully control the synthesis of telechelic star polymers, and various experiments have been performed on solutions of telechelic star polymers at finite density [24,25] showing an extremely interesting aggregation scenario. With this study we have established telechelic star polymers as a novel, promising, and extremely versatile self-assembled and tunable patchy particle system. The capability of these macromolecules to self-assemble into robust, soft patchy particles that maintain their shape and directionality deep into the semidilute regime, surpasses problems related to the fabrication of conventional patchy colloids, opening-up ample new opportunities for experiments and technological applications. Their flexibility, which stems from their soft nature as fluctuating polymers, selectively stabilizes target crystals for a broad range of concentrations, opening the way for the self-assembly of a variety of desired solids.

We thank Dimitris Vlassopoulos (Heraklion, Greece) for useful comments and suggestions and Emanuela Bianchi (Vienna, Austria) for useful discussions. This work was partially supported by the Marie Curie ITN-COMPLOIDS (Grant Agreement No. 234810). Computer time at the Vienna Scientific Cluster (VSC) is gratefully acknowledged.

*Corresponding author.

†barbara.capone@univie.ac.at

- [1] S. C. Glotzer and M. J. Solomon, *Nat. Mater.* **6**, 557 (2007).
- [2] S. Angioletti-Uberti, B. M. Mognetti, and D. Frenkel, *Nat. Mater.* **11**, 518 (2012).
- [3] S. Torquato and Y. Jiao, *Nature (London)* **460**, 876 (2009).
- [4] F. Romano, E. Sanz, and F. Sciortino, *J. Chem. Phys.* **132**, 184501 (2010).
- [5] P. Akcora *et al.*, *Nat. Mater.* **8**, 354 (2009).
- [6] C. E. Snyder, A. M. Yake, J. D. Feick, and D. Velegol, *Langmuir* **21**, 4813 (2005).
- [7] A. M. Yake, C. E. Snyder, and D. Velegol, *Langmuir* **23**, 9069 (2007).
- [8] Z. Nie, W. Li, M. Seo, S. Xu, and E. Kumacheva, *J. Am. Chem. Soc.* **128**, 9408 (2006).
- [9] A. B. Pawar and I. Kretzschmar, *Langmuir* **24**, 355 (2008).
- [10] A. B. Pawar and I. Kretzschmar, *Langmuir* **25**, 9057 (2009).
- [11] F. Lo Verso, C. N. Likos, C. Mayer, and H. Löwen, *Phys. Rev. Lett.* **96**, 187802 (2006).
- [12] F. Lo Verso, A. Z. Panagiotopoulos, and C. N. Likos, *Faraday Discuss.* **144**, 143 (2010).
- [13] E. Bianchi, R. Blaak, and C. N. Likos, *Phys. Chem. Chem. Phys.* **13**, 6397 (2011).
- [14] B. Capone, J.-P. Hansen, and I. Coluzza, *Soft Matter* **6**, 6075 (2010).
- [15] See Supplemental Material at <http://link.aps.org/supplemental/10.1103/PhysRevLett.109.238301> for the details on the coarse graining techniques and on the data analysis methodology.
- [16] B. Capone, I. Coluzza, and J.-P. Hansen, *J. Phys. Condens. Matter* **23**, 194102 (2011).
- [17] B. M. Ladanyi and D. Chandler, *J. Chem. Phys.* **62**, 4308 (1975).
- [18] F. Lo Verso, C. N. Likos, and H. Löwen, *J. Phys. Chem. C* **111**, 15 803 (2007).
- [19] J. Zhang, Z.-Y. Lu, and S. Zhao-Yan, *Soft Matter* **7**, 9944 (2011).
- [20] G. Srinivas and J. W. Pitera, *Nano Lett.* **8**, 611 (2008).
- [21] E. G. Noya, C. Vega, J. P. K. Doye, and A. A. Louis, *J. Chem. Phys.* **132**, 234511 (2010).
- [22] E. Bianchi, J. Largo, P. Tartaglia, E. Zaccarelli, and F. Sciortino, *Phys. Rev. Lett.* **97**, 168301 (2006).
- [23] J. Russo, J. M. Tavares, P. I. C. Teixeira, M. M. Telo da Gama, and F. Sciortino, *Phys. Rev. Lett.* **106**, 085703 (2011).
- [24] D. B. Alward, D. J. Kinning, E. L. Thomas, and L. J. Fetters, *Macromolecules* **19**, 215 (1986).
- [25] E. L. Thomas, D. B. Alward, D. J. Kinning, D. C. Martin, D. L. Handlin Jr., and L. J. Fetters, *Macromolecules* **19**, 2197 (1986).